Numerical modeling of whispering gallery waves in elastic multilayered spheres

Matthieu Gallezot, Fabien Treyssède, Odile Abraham

Université de Nantes, GeM
Univ Gustave Eiffel, campus de Nantes, IFSTTAR, GERS-GeoEND

GIS ECND-PdL webinar
June 22, 2022

Outline

1. Introduction
2. Numerical model
3. Numerical results
4. Conclusion

Goal

Whispering gallery waves:

- Optics: well-known, modes confined near surface+equator, high quality factor
- Elasticity: analogy? differences?

→ Let us compute the resonances (vibration modes) of a buried elastic sphere...

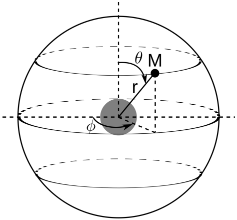

Issues:

- efficient high-frequency model: no full 3D, no full analytical (unstable)[1] → **1D semi-analytical FE model**

[1] V. Dubrovskiy and V. Morochnik (1981), *Izv. Earth Phys* 17

Goal

Whispering gallery waves:

- Optics: well-known, modes confined near surface+equator, high quality factor
- Elasticity: analogy? differences?

→ Let us compute the resonances (vibration modes) of a buried elastic sphere...

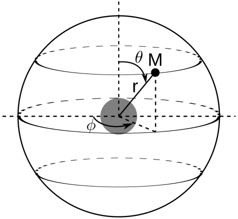

Issues:

- efficient high-frequency model: no full 3D, no full analytical (unstable)[1] → **1D semi-analytical FE model**
- resonances of open systems: unbounded problem, leaky resonances ('improper' modes growing at infinity[2]) → **Perfectly Matched Layer truncation** (PML)

[1] V. Dubrovskiy and V. Morochnik (1981), *Izv. Earth Phys* 17

[2] P. Lalanne, W. Yan, K. Vynck, C. Sauvan, and J.-P. Hugonin (2018), *Laser & Photonics Reviews* 12 ; M. Mansuripur, M. Kolesik, and P. Jakobsen (2017), *Phys. Rev. A* 96 (1) ; M. Gallezot (2018), PhD thesis, Ecole Centrale Nantes

Outline

1 Introduction

2 Numerical model
- The elastodynamic problem
- Analytical description of the angular behaviour
- Semi-analytical finite element formulation
- Resonances and forced response

3 Numerical results

4 Conclusion

Weak form of the elastodynamic problem truncated with a radial PML

Weak form of elastodynamics in spherical coordinates:

$$\int_{\tilde{V}} \delta\tilde{\epsilon}^{\mathrm{T}}\tilde{\boldsymbol{\sigma}}\mathrm{d}\tilde{V} - \omega^2 \int_{\tilde{V}} \tilde{\rho}\delta\tilde{\boldsymbol{u}}^{\mathrm{T}}\tilde{\boldsymbol{u}}\mathrm{d}\tilde{V} = \int_{\tilde{V}} \delta\tilde{\boldsymbol{u}}^{\mathrm{T}}\tilde{\boldsymbol{f}}\mathrm{d}\tilde{V} + \int_{\partial\tilde{V}} \delta\tilde{\boldsymbol{u}}^{\mathrm{T}}\tilde{\boldsymbol{t}}\mathrm{d}\partial\tilde{V} \quad (1)$$

- $\tilde{\boldsymbol{u}}(r,\theta,\phi) = \left[\tilde{u}_r(\tilde{r},\theta,\phi),\ \tilde{u}_\theta(\tilde{r},\theta,\phi),\ u_\phi(\tilde{r},\theta,\phi)\right]^{\mathrm{T}}$, $\mathrm{d}\tilde{V} = \tilde{r}^2 \sin\theta \mathrm{d}\tilde{r}\mathrm{d}\theta\mathrm{d}\phi$
- $\tilde{\epsilon} = \tilde{\boldsymbol{L}}\tilde{\boldsymbol{u}}$ where $\tilde{\boldsymbol{L}} = \boldsymbol{L}_r \frac{\partial}{\partial\tilde{r}} + \boldsymbol{L}_\theta \frac{\partial}{\tilde{r}\partial\theta} + \boldsymbol{L}_\phi \frac{\partial}{\tilde{r}\sin\theta\partial\phi} + \frac{1}{\tilde{r}}\boldsymbol{L}_1 + \frac{\cot\theta}{\tilde{r}}\boldsymbol{L}_2$
- $\tilde{r} \mapsto r$ i.e. $\tilde{g}(\tilde{r}) = g(r),\ \partial\tilde{g}/\partial\tilde{r} = \partial g/(\gamma(r)\partial r),\ \mathrm{d}\tilde{r} = \gamma(r)\mathrm{d}r$
- assumption: transverse isotropic materials

Truncature with a radial PML

PML $\equiv$ analytic continuation[a] of the radial coordinate

$$\tilde{r}(r) = \int_0^r \gamma(\xi)\mathrm{d}\xi, \quad (2)$$

with the attenuation function

- $\gamma(r) = 1$ if $r < d$,
- $\mathbf{Im}\ \boldsymbol{\gamma(r) > 0}$ if $d < r < d + h$.

[a] W. C. Chew and W. H. Weedon (1994), *Microwave and Optical Technology Letters 7*

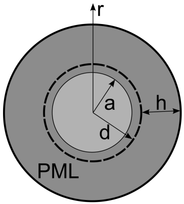

Analytical description of the angular behaviour (θ, ϕ)

The angular and radial variables can be separated:

$$\boldsymbol{u}(r,\theta,\phi) = \sum_{l\geq 0} \sum_{|m|\leq l} \boldsymbol{S}_l^m(\theta,\phi)\hat{\boldsymbol{u}}_l^m(r) \quad (3)$$

A. C. Eringen and E. S. Şuhubi (1975), vol. II, Academic Press ; E. Kausel (2006), Cambridge University Press

Matrix of vector spherical harmonics

$$\boldsymbol{S}_l^m(\theta,\phi) = \begin{bmatrix} \mathrm{Y}_l^m(\theta,\phi) & 0 & 0 \\ 0 & \frac{\partial \mathrm{Y}_l^m(\theta,\phi)}{\partial\theta} & -\frac{\partial \mathrm{Y}_l^m(\theta,\phi)}{\sin\theta\partial\phi} \\ 0 & \frac{\partial \mathrm{Y}_l^m(\theta,\phi)}{\sin\theta\partial\phi} & \frac{\partial \mathrm{Y}_l^m(\theta,\phi)}{\partial\theta} \end{bmatrix}. \quad (4)$$

with the scalar spherical harmonics

$$Y_l^m(\theta,\phi) = \sqrt{\frac{(2l+1)(l-m)!}{4\pi(l+m)!}} P_l^m(\cos\theta)\mathrm{e}^{\mathrm{j}m\phi}, \; l\in\mathbb{N}, \; |m|\leq l. \quad (5)$$

$P_l^m(\cos\theta)$: associated Legendre polynomial, (l,m): polar and azimuthal wavenumbers

Finite element discretization of the radial coordinate:

$$\hat{\boldsymbol{u}}_l^{m,e}(r) = \boldsymbol{N}^e(r)\hat{\boldsymbol{U}}_l^{m,e}, \quad \delta\boldsymbol{u}^{\mathrm{T}}(r,\theta,\phi) = \delta\hat{\boldsymbol{U}}^{e\mathrm{T}}\boldsymbol{N}^{e\mathrm{T}}(r)\boldsymbol{S}_k^{p*}(\theta,\phi) \quad (6)$$

Angular integration of the weak formulation

Angular integration strategies:

1. Numerical integration (P. Heyliger and A Jilani (1992), *International Journal of Solids and Structures* 29)
2. Manual integration for a specific choice of interpolation function (J. Park (2002), PhD thesis, Massachusetts Institute of Technology)
3. **Use orthogonality relations of Spherical Harmonics** thanks to the choice of $\delta \boldsymbol{u}$

Angular integration of the weak formulation

Angular integration strategies:

3. **Use orthogonality relations of Spherical Harmonics** thanks to the choice of $\delta\boldsymbol{u}$

Orthogonality

- "Classical" orthogonality of vector SH (E. Kausel (2006), Cambridge University Press):

$$\int_0^{\pi}\int_0^{2\pi} \boldsymbol{S}_k^{p*}\,\boldsymbol{S}_l^m \mathrm{d}\phi \sin\theta \mathrm{d}\theta = \begin{bmatrix} 1 & 0 & 0 \\ 0 & \bar{l} & 0 \\ 0 & 0 & \bar{l} \end{bmatrix} \delta_{kl}\delta_{mp}, \quad \text{with } \bar{l} = l(l+1) \qquad (7)$$

$\rightarrow$ harmonics uncoupled in the mass term (kinetic energy)

- "Painful" orthogonality of **tensor SH** (Z. Martinec (2000), *Geophysical Journal International* 142), *e.g.* for one component:

$$\int_0^{\pi}\int_0^{2\pi} \left[\left(\frac{\partial^2 Y_k^{p*}}{\partial\theta^2} - \cot\theta \frac{\partial Y_k^{p*}}{\partial\theta} - \frac{1}{\sin^2\theta}\frac{\partial^2 Y_k^{p*}}{\partial\phi^2} \right) \left(\frac{\partial^2 Y_l^{m}}{\partial\theta^2} - \cot\theta \frac{\partial Y_l^{m}}{\partial\theta} - \frac{1}{\sin^2\theta}\frac{\partial^2 Y_l^{m}}{\partial\phi^2} \right) + 4\frac{\partial}{\partial\theta}\left(\frac{1}{\sin\theta}\frac{\partial Y_k^{p*}}{\partial\phi}\right)\frac{\partial}{\partial\theta}\left(\frac{1}{\sin\theta}\frac{\partial Y_l^{m}}{\partial\phi}\right) \right] \mathrm{d}\phi \sin\theta \mathrm{d}\theta = (l-1)\bar{l}(l+2)\delta_{kl}\delta_{mp}, \qquad (8)$$

$\rightarrow$ harmonics uncoupled in the stiffness term (elastic potential energy)

The 1D semi-analytical finite element formulation

After tedious algebraic manipulations...

Finite element system

$$\left(\boldsymbol{K}(l) - \omega^2 \boldsymbol{M}(l)\right) \hat{\boldsymbol{U}}_l^m = \hat{\boldsymbol{F}}_l^m \tag{9}$$

with $\boldsymbol{K}(l) = \boldsymbol{K}_1(l) + \boldsymbol{K}_2(l) + \boldsymbol{K}_2^{\mathrm{T}}(l) + \boldsymbol{K}_3(l)$ and:

$$\boldsymbol{K}_1^e(l) = \int \frac{\mathrm{d}\boldsymbol{N}^{e\mathrm{T}}}{\mathrm{d}r} \begin{bmatrix} C_{11} & 0 & 0 \\ 0 & \bar{l}C_{55} & 0 \\ 0 & 0 & \bar{l}C_{55} \end{bmatrix} \frac{\mathrm{d}\boldsymbol{N}^e}{\mathrm{d}r} \frac{\tilde{r}^2}{\gamma} \mathrm{d}r \,, \tag{10}$$

$$\boldsymbol{K}_2^e(l) = \int \frac{\mathrm{d}\boldsymbol{N}^{e\mathrm{T}}}{\mathrm{d}r} \begin{bmatrix} 2C_{12} & -\bar{l}C_{12} & 0 \\ \bar{l}C_{55} & -\bar{l}C_{55} & 0 \\ 0 & 0 & -\bar{l}C_{55} \end{bmatrix} \boldsymbol{N}^e \tilde{r} \mathrm{d}r \,, \tag{11}$$

$$\boldsymbol{K}_3^e(l) = \int \boldsymbol{N}^{e\mathrm{T}} \begin{bmatrix} \bar{l}C_{55} + 4C_\beta & -\bar{l}(C_{55} + 2C_\beta) & 0 \\ -\bar{l}(C_{55} + 2C_\beta) & \bar{l}(C_{55} + \bar{l}C_{23} + 2(\bar{l} - 1)C_{44}) & 0 \\ 0 & \bar{l}(C_{55} + (\bar{l} - 2)C_{44}) & 0 \end{bmatrix} \boldsymbol{N}^e \gamma \mathrm{d}r \,, \tag{12}$$

$$\boldsymbol{M}^e(l) = \int \rho \boldsymbol{N}^{e\mathrm{T}} \begin{bmatrix} 1 & 0 & 0 \\ 0 & \bar{l} & 0 \\ 0 & 0 & \bar{l} \end{bmatrix} \boldsymbol{N}^e \tilde{r}^2 \gamma \mathrm{d}r \qquad (\text{with } C_\beta = C_{23} + C_{44}) \tag{13}$$

- Fully analytical description along the angular coordinate for any type of FE interpolation → easy to implement
- Finite element is 1D → fast computations

Resonances and forced response

Resonances: free response

$$\left(\boldsymbol{K}(l) - \omega_l^2 \boldsymbol{M}(l)\right) \hat{\boldsymbol{U}}_l^m = \boldsymbol{0} \tag{14}$$

- **Linear** eigenproblem $\rightarrow$ simple to solve
- The resonances $\omega_l^{(n)}$ and radial modeshapes $\hat{\boldsymbol{U}}_l^{(n)}$ depend on l
- ... but not on the azimuthal wavenumber m (for a given l, $2l+1$ modes with the same eigenfrequency)

Resonances and forced response

Resonances: free response

$$\left(\boldsymbol{K}(l) - \omega_l^2 \boldsymbol{M}(l)\right) \hat{\boldsymbol{U}}_l^m = \boldsymbol{0} \tag{14}$$

- **Linear** eigenproblem $\rightarrow$ simple to solve
- The resonances $\omega_l^{(n)}$ and radial modeshapes $\hat{\boldsymbol{U}}_l^{(n)}$ depend on l
- ... but not on the azimuthal wavenumber m (for a given l, $2l+1$ modes with the same eigenfrequency)

Forced response ($\hat{\boldsymbol{F}}_l^m \neq \boldsymbol{0}$)

- $\boldsymbol{K}$, $\boldsymbol{M}$ are complex but symmetric $\rightarrow$ straightforward **modal orthogonalty**
- Modal superposition leads to:

$$\boldsymbol{U}(\theta, \phi, t) = \sum_{l \geq 0} \sum_{|m| \leq l} \boldsymbol{S}_l^m(\theta, \phi) \frac{1}{2\pi} \int_{-\infty}^{+\infty} \left[\sum_{n=1}^{N} \frac{\hat{\boldsymbol{U}}_l^{(n)\mathrm{T}} \hat{\boldsymbol{F}}_l^m(\omega) \hat{\boldsymbol{U}}_l^{(n)}}{\omega_l^{(n)2} - \omega^2} \right] \mathrm{e}^{-\mathrm{j}\omega t} \mathrm{d}\omega. \tag{15}$$

Resonances and forced response

Resonances: free response

$$\left(\boldsymbol{K}(l) - \omega_l^2 \boldsymbol{M}(l)\right) \hat{\boldsymbol{U}}_l^m = \boldsymbol{0} \tag{14}$$

- **Linear** eigenproblem $\rightarrow$ simple to solve
- The resonances $\omega_l^{(n)}$ and radial modeshapes $\hat{\boldsymbol{U}}_l^{(n)}$ depend on l
- … but not on the azimuthal wavenumber m (for a given l, $2l+1$ modes with the same eigenfrequency)

Forced response ($\hat{\boldsymbol{F}}_l^m \neq \boldsymbol{0}$)

- $\boldsymbol{K}$, $\boldsymbol{M}$ are complex but symmetric $\rightarrow$ straightforward **modal orthogonalty**
- Modal superposition leads to:

$$\boldsymbol{U}(\theta,\phi,t) = \sum_{l\geq 0}\sum_{|m|\leq l} \boldsymbol{S}_l^m(\theta,\phi) \frac{1}{2\pi}\int_{-\infty}^{+\infty}\left[\sum_{n=1}^{N} \frac{\hat{\boldsymbol{U}}_l^{(n)\mathrm{T}} \hat{\boldsymbol{F}}_l^m(\omega) \hat{\boldsymbol{U}}_l^{(n)}}{\omega_l^{(n)2} - \omega^2}\right] \mathrm{e}^{-\mathrm{j}\omega t} \mathrm{d}\omega. \tag{15}$$

$\hat{\boldsymbol{F}}_l^m(\omega)$: force coefficients obtained from the vector SH transform of $\boldsymbol{F}(\theta,\phi,\omega)$
$\hat{\boldsymbol{F}}_l^m(\omega) = \int_0^\pi \int_0^{2\pi} \boldsymbol{S}_l^{m*}(\theta,\phi)\boldsymbol{F}(\theta,\phi,\omega)\mathrm{d}\phi \sin\theta \mathrm{d}\theta$ $\rightarrow$ fast tools needed!
Numerical integration strategy: FFT for ϕ + GLQ for $\cos\theta$ (see M. A. Wieczorek and M. Meschede (2018), *Geochemistry, Geophysics, Geosystems* 19)

Outline

1 Introduction

2 Numerical model

3 Numerical results
- Validation: surface-free homogeneous sphere
- Generation of whispering-gallery waves
- Resonances of a buried sphere

4 Conclusion

Resonances of a surface-free sphere

Reference results for a homogeneous, isotropic, surface-free sphere: A. C. Eringen and E. S. Șuhubi (1975), vol. II, Academic Press (black curves).
Numerical model: no PML, 1014 dofs (quadratic 1D finite elements).

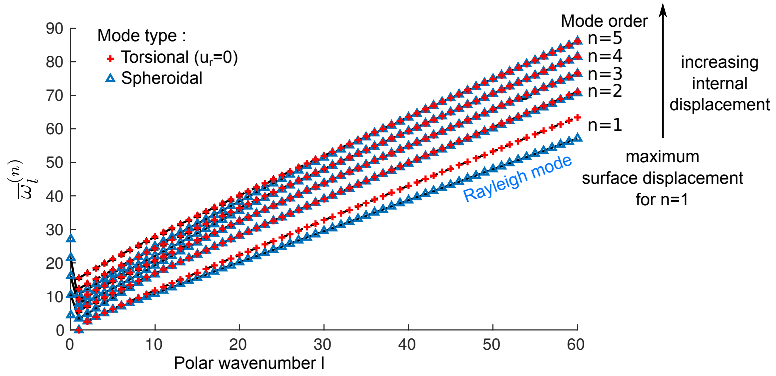

Resonances of a surface-free sphere

Reference results for a homogeneous, isotropic, surface-free sphere: A. C. Eringen and E. S. Şuhubi (1975), vol. II, Academic Press (black curves).
Numerical model: no PML, 1014 dofs (quadratic 1D finite elements).

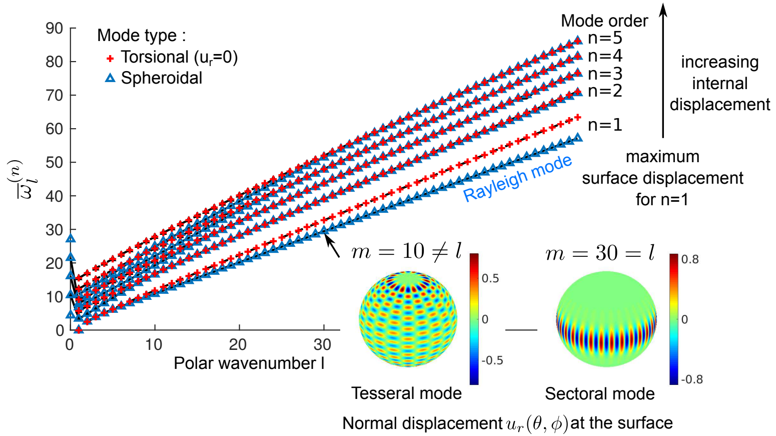

Generation of whispering-gallery waves

Polar aperture of line source for a collimating (diffraction-free) Rayleigh wave (D. Clorennec and D. Royer (2004), *Applied physics letters* 85):

$$\theta_{\mathrm{COL}} = \sqrt{\frac{\pi c_R}{4 a f_c}}$$

(if $\theta > \theta_{\mathrm{COL}}$: focusing, if $\theta < \theta_{\mathrm{COL}}$: diverging)

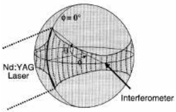

Forced response model: superposition on $N = 80$ eigenmodes for $l = 0$ to $l = 150$, viscoelastic steel (c_R=2919.8m/s), radius a=25mm, f_c=1MHz $\Rightarrow \theta_{\mathrm{COL}} \approx 17^\circ$

Generation of whispering-gallery waves

Polar aperture of line source for a collimating (diffraction-free) Rayleigh wave (D. Clorennec and D. Royer (2004), *Applied physics letters* 85):

$$\theta_{\mathrm{COL}} = \sqrt{\frac{\pi c_R}{4 a f_c}}$$

(if $\theta > \theta_{\mathrm{COL}}$: focusing, if $\theta < \theta_{\mathrm{COL}}$: diverging)

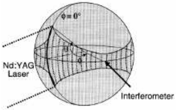

Forced response model: superposition on $N = 80$ eigenmodes for $l = 0$ to $l = 150$, viscoelastic steel (c_R=2919.8m/s), radius a=25mm, f_c=1MHz $\Rightarrow \theta_{\mathrm{COL}} \approx 17^\circ$

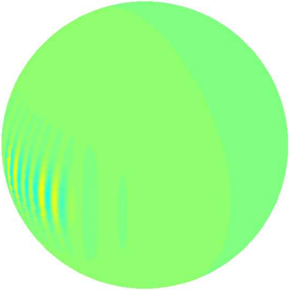

Modal analysis:

- modes are spheroidal (radial source)
- leading wavenumbers: sectoral ($m \approx l$)
- dominant mode = Rayleigh wave ($n = 1$) ($n > 1$ modes $\equiv$ body waves)

Adding a coating layer

Let us add a 1mm layer of viscoelastic epoxy at the surface of the sphere...

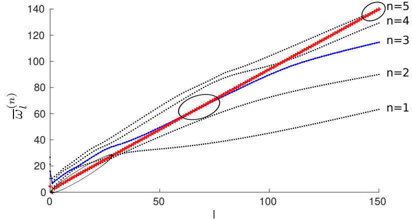

Eigenfrequencies of the coated sphere (red: Rayleigh mode without coating)

- Collimating wave is possible at the sphere-coating interface
- ... but the Rayleigh-like behavior depends on the frequency (dispersion) $\rightarrow$ the source must be designed accordingly: f_c=1.2MHz, $\theta_{COL} \approx 15^\circ$

Adding a coating layer

Let us add a 1mm layer of viscoelastic epoxy at the surface of the sphere...

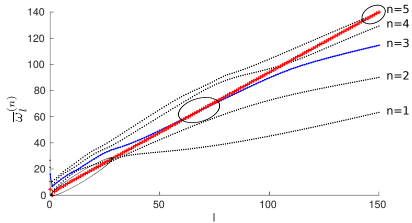

Eigenfrequencies of the coated sphere (red: Rayleigh mode without coating)

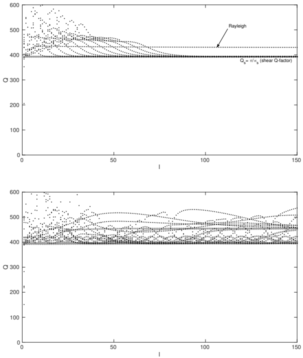

Quality factors $Q = -\mathrm{Re}\,\omega / 2\mathrm{Im}\,\omega$. Top: sphere, bottom: coated sphere (gray: torsional modes)

- Collimating wave is possible at the sphere-coating interface
- ... but the Rayleigh-like behavior depends on the frequency (dispersion)
  $\rightarrow$ the source must be designed accordingly: f_c=1.2MHz, $\theta_{\mathrm{COL}} \approx 15^\circ$
- The Q-factors ∼decrease toward the shear or Rayleigh Q-factors (∼400 for steel)

Resonances of a steel sphere buried in concrete

PML parameters: complex thickness $\hat{\gamma} \times h = (1 + 2\mathrm{j}) \times 0.25a$, $d = a$

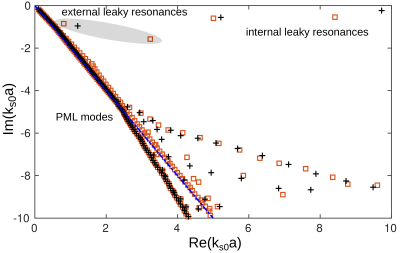

Typical spectrum of a buried sphere: discrete leaky poles + continua of radiation modes PML-rotated by $-\arg\hat{\gamma}$ (black:torsional, red: spheroidal)

- Filtering of radiation modes required

Resonances of a steel sphere buried in concrete

PML parameters: complex thickness $\hat{\gamma} \times h = (1 + 2\mathrm{j}) \times 0.25a$, $d = a$

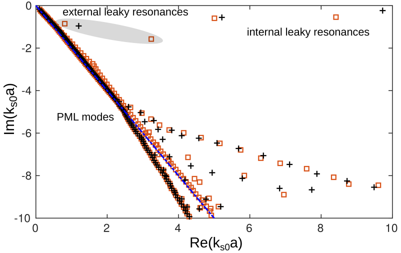

Typical spectrum of a buried sphere: discrete leaky poles + continua of radiation modes PML-rotated by $-\arg\hat{\gamma}$ (black:torsional, red: spheroidal)

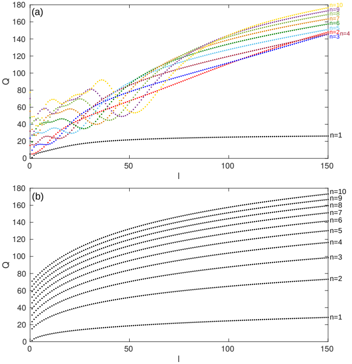

Q-factors (top: spheroidal, bottom: torsional)

- Filtering of radiation modes required
- The Q-factor tends to increase with frequency (probably up to $Q_{R,s}$)
- Significant reduction of Q-factors (energy leakage)
- The Rayleigh mode has the worst Q-factor

Outline

1. Introduction
2. Numerical model
3. Numerical results
4. Conclusion

Conclusion

A general numerical model for multi-layered buried elastic spheres:

- easy to implement (tensor SH orthogonality)
- fast building of FE matrices (1D finite element)
- fast computation of resonances (linear eigenproblem)
- fast calculation of the forced response (post-processing using mode orthogonality)

Results:

- accuracy checked by comparison with literature results
- collimating Rayleigh wave experiment is recovered numerically
- modal formalism is mandatory due to multimodal and dispersive nature of waves
- quality factors: much weaker than in optics

Future works:

- experiments (on-going, in collaboration with A. Duclos, LAUM)
- design of geometry and materials?
- sensor prototyping...

Thank you for your attention

Transient signals

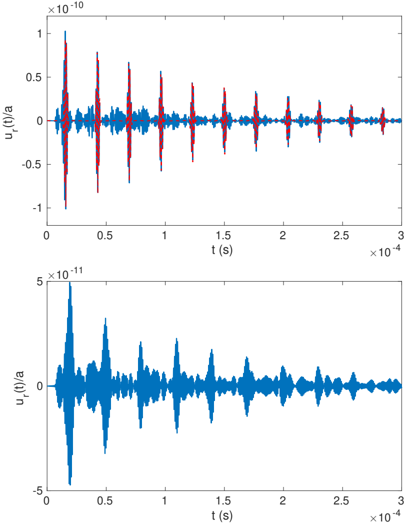

Transient signals at $\theta = 90^{\circ}$ and $\phi = \pi/2$. Superposition on N=80 eigenmodes. Top: sphere (red: superposition on the Rayleigh mode only), bottom: coated sphere.

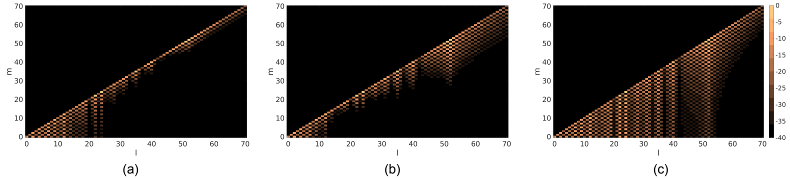

Forced response $10\log_{10}(|\hat{u}_l^m/\max\ \hat{u}_l^m|)$ (dB) at the surface of a viscoelastic sphere ($r = a$) and at the centre frequency ($\overline{\omega} = 49.46$) for (a) a collimating wave ($\theta_\sigma = 0.1514$); (b) a focusing wave ($\theta_\sigma = 0.2668$); (c) a diverging wave ($\theta_\sigma = 0.0667$).

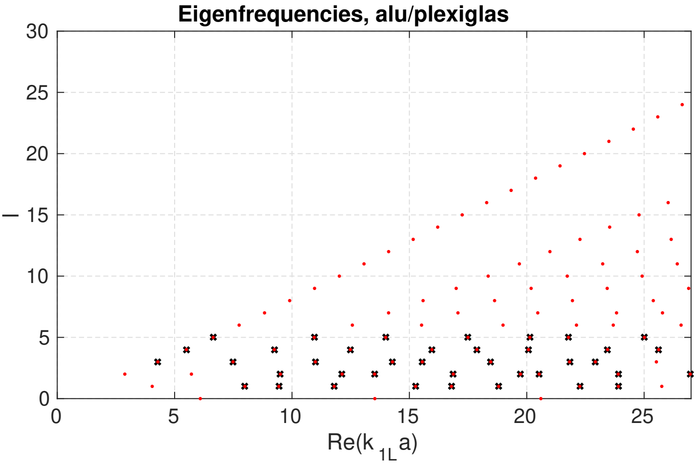

Aluminium sphere into plexiglas matrix. Black: J.-P. Sessarego, J. Sageloli, R. Guillermin, and H. Überall (1998), *The Journal of the Acoustical Society of America* 104 results; Red: numerical results. PML parameters: $h = 0.5a$, $d = a$, $\hat{\gamma} = 2 + 4\mathrm{j}$.